JOURNAL OF MATERIALS SCIENCE 31 (1996) 2833-2838

Synthesis and characterization of CaO-stabilized ZrO_2 fine powders for oxygen ionic conductors

JOO-SIN LEE, JUNG-IL PARK, TAE-WOON CHOI
Kyung-Sung University, Department of Materials Science and Engineering, Pusan, 608-736, Republic of Korea

13 mol% calcia-stabilized zirconia (CSZ) powders were synthesized by the coprecipitation method. The characterization of powders has been investigated using thermogravimetry and differential thermal analysis for thermal analysis, X-ray diffraction and infrared spectroscopy for crystalline phases identification, Brunauer–Emmett–Teller, X-ray diffraction-line broadening and transmission electron microscopy (TEM) for particle size and morphology determination. The characteristics of powders prepared by the coprecipitation method are discussed.

1. Introduction

Stabilized zirconia introduced di- or tri-valent oxides, such as CaO, MgO and Y_2O_3, have historically received the most attention as solid electrolyte membranes in electrochemical devices, such as oxygen sensors, fuel cells, and oxygen pumps. For applications in such devices it is important that the materials have good ionic conductivity ($> 10^{-2}\,\Omega^{-1}\,cm^{-1}$ at the operating temperature), that they are ionic conductors (transport number $t_i > 0.99$) over a wide range of oxygen partial pressures, and are impermeable to prevent direct molecular transport of oxygen through the materials (density $> 92\%$) [1].

Among these requirements, in order to prevent leakage of gas consisting of oxygen, a high-density sintered body must be fabricated economically. However, if conventional ceramic processing methods are employed in which ball-milled powders of the pure component oxides are mixed, die-pressed, and calcined, a dense zirconia cannot be fabricated easily. Therefore, other methods are introduced: the use of fine powders, the use of additives, the use of hot-pressing, and so on.

The synthesis of fine powders to obtain a dense sintered body was investigated in this study. Fine powders improve the sinterability at lower temperatures and/or shorter times than coarse ones, because there is more surface area per unit volume and because transport distances are shorter. The present study focused on the powder characteristics prepared by the coprecipitation method, which is the most convenient way to prepare fine powders from aqueous solution. The 13 mol % CaO–ZrO_2 gels were precipitated with $(NH_4)_2C_2O_4H_2O$ and NH_4OH from mixed aqueous solutions of $ZrCl_4$ and $CaCl_2$. After drying and calcination of the precipitates, the phase transitions with the calcination temperatures, crystallization temperature, and quantitative relations of the phases, were investigated by X-ray diffraction (XRD) and infrared spectroscopy (IR) measurements.

The formation of hard agglomerates should be suppressed in order to promote the sintering density in terms of a homogeneous microstructure. To avoid the formation of agglomerates, a washing process with ethyl alcohol, a stirring process during washing, and a milling process after calcination, were employed. The most important parameter for powders is the particle size, including the primary particle (or crystallite) size and the secondary particle (agglomerate) size. The particle size has an important effect on the phase transitions, compaction, and sinterability of powders, so its determination is of importance. In the present study, particle size and morphology were determined using Brunauer–Emmett–Teller (BET), X-ray diffraction-line broadening (XRD-LB) and transmission electron microscopy (TEM) techniques. The preparation and characterization of CaO-stabilized ZrO_2 fine powders to fabricate dense materials for use as oxygen ionic conductors are described.

2. Experimental procedure

2.1. Powder preparation

Powders of calcia-stabilized zirconia were synthesized by the coprecipitation method. A composition corresponding to 13 mol % CaO–ZrO_2 was prepared from an aqueous solution of high purity $ZrCl_4$ powder (Aldrich Chemical Co., 99.5%) and $CaCl_2$ powder (Aldrich Chemical Co., 97%), and coprecipitated with an aqueous solution of $(NH_4)_2C_2O_4H_2O$ powder (Junsei Chemical Co., 99.5%) and NH_4OH (Junsei Chemical Co., NH_3 28%–30%). The precipitate was a mixture of $Zr(OH)_4$ and $CaC_2O_4H_2O$.

The precipitates were washed with distilled water three times to remove chloride ions, followed by washing with ethyl alcohol three times to lighten the

0022–2461 © *1996 Chapman & Hall*

agglomeration effect. The powders were cleaned and dispersed in an ultrasonic cleaner under vigorous stirring. They were then filtered and dried. It is well known that the agglomeration behaviour of ceramic powders is influenced by the washing process. For the preparation of stabilized zirconia powders, it has been demonstrated previously [2,3] that the powders washed with alcohol before drying show the formation of weak agglomerates due to the lower surface tension of alcohol than those washed with water.

Drying was performed at about 120 °C in a drying oven for 10 h. Dried powders were stored in a desiccator to prevent the contamination with H_2O or CO_2 from air. After drying, the material was calcined for 30 min at different temperatures from 400–1400 °C with intervals of 100 °C. To eliminate agglomerates produced in the calcination process, the powders calcined from 700–1000 °C were ball milled in ethanol for 24 h. For milling, a plastic jar and zirconia balls were used. The drying process was then introduced again. After drying the material was screened with a seive of 325 mesh.

2.2. Characterization techniques

The characterization of powders was performed using thermogravimetric analysis (TG), differential thermal analysis (DTA), X-ray diffraction (XRD), Brunauer–Emmett–Teller (BET), infrared (IR) spectroscopy, transmission electron microscopy (TEM) methods.

Thermal analysis was performed on the coprecipitated powders at a heating rate of 10 °C min^{-1} by using TG and DTA (Seiko Instruments Inc.).

The phase transitions with the calcination temperatures were determined by XRD and IR measurements. Standard X-ray diffractometry (Rigaku Denki Co.) using nickel-filtered $\text{Cu}K_\alpha$ radiation was used to identify crystalline phases. The X-ray patterns were recorded in the range $20° < 2\theta < 80°$. Infrared spectra were obtained with a Nicolet Company System 800 infrared spectrophotometer. Powder absorption spectra were taken by using the pellets of 0.67 wt % zirconia in KBr.

Primary particle size and crystallite size were determined with BET, XRD-LB and TEM techniques. The specific surface area was measured by the multipoint BET (Quantachrome Corp., Quantasorb-17) method using nitrogen gas as the absorbate. The average particle size was calculated from the equation

$$d = \frac{6}{\rho A} \tag{1}$$

where d is the average particle size (cm), ρ is the theoretical density of the sample (g cm^{-3}), and A is the specific surface area (m^2g^{-1}). The particles were assumed to be spheres, and the theoretical density used a value of 5.636 g cm^{-3}. It was calculated assuming the oxygen vacancy model for 13 mol % CaO in ZrO_2.

For the estimation of crystallite sizes as a function of calcination temperature, X-ray diffraction-line broadening (XRD-LB) measurements have also been performed. The Scherrer equation was used for the calculation:

$$D = \frac{k\lambda}{B\ \cos\theta} \tag{2}$$

where D is the crystallite size (nm), λ is the wavelength of $\text{Cu}K_\alpha$ radiation (nm), θ is the Bragg angle (deg), k is a constant, 0.89, and B is the calibrated breadth of a diffraction peak at half-maximum intensity (rad).

Assessments of particle size and the state of agglomeration were obtained from TEM observations (Jeol Co., JEM-100S). Powders were dispersed in ethyl alcohol using an ultrasonic treatment for 10 min to prepare a dilute suspension before sampling. The samples were introduced on to a formvar grid for TEM observations.

3. Results and discussion

After drying of the precipitates washed with ethyl alcohol, BET and TEM measurements were performed to estimate particle size and morphology of the precipitates. The specific surface area of precipitates according to the BET method was 193 $\text{m}^2\,\text{g}^{-1}$, and the average particle size was approximately 5 nm. Estimates of particle sizes from a transmission electron micrograph were in reasonable agreement with the results of BET method. These precipitates appear to be the fine and spherical primary particles with a size of approximately 5 nm.

After drying of the precipitates, TG and DTA were carried out between room temperature and 1300 °C. Fig. 1 shows the TG and DTA curves of the precipitated powders measured with a heating rate of 10 °C min^{-1}. Peaks related to the evaporation and combustion of alcohol and the evaporation of residual water in low-temperature regions are seen. An exothermic peak at 462 °C can be attributed to the decomposition of calcium oxalate ($CaC_2O_4 \rightarrow CaCO_3 + CO$) and the crystallization of zirconia. Probably due to the decarbonation of the carbonate, an endothermic peak is observed around 666 °C (see XRD data of Fig. 2). After the endothermic peak no other thermal effect is observed up to 1300 °C.

The dried powders were calcined for 30 min at temperatures ranging from 400–1400 °C with intervals of 100 °C. The powders were heated at a heating rate of

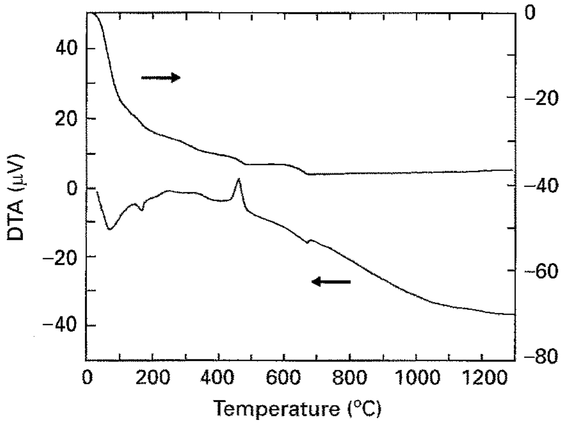

Figure 1 TG and DTA curves of the precipitates dried at 120 °C.

$10\,^{\circ}\mathrm{C\,min}^{-1}$ and cooled to room temperature in the furnace. The phase transitions occurring with calcination temperatures have been studied by XRD and IR measurements. The amount of the phases, in addition to the phase identification, can also be estimated quantitatively by XRD analysis.

Fig. 2 shows XRD patterns obtained from different thermal treatments. The material calcined at 400 °C shows the amorphous state, but is transformed at 500 °C to the tetragonal crystalline structure, although the diffraction pattern is rather wide and spreading, indicating a poor crystallinity.

At 500 °C, major peaks of tetragonal phase (111, 202, 131 and 200 planes in decreasing intensity) appear, and the calcium carbonate $CaCO_3$ (calcite) peak appears near the main peak of the tetragonal phase (111 plane). From this, it can be identified that the strong exothermic peak at 462 °C in DTA is due to the formation of calcium carbonate and the crystallization of amorphous phase.

In addition to the tetragonal phase and the calcium carbonate phase, a little monoclinic phase exists at around 500 and 600 °C. At 700 °C, the intensity of all the tetragonal peaks becomes weaker in comparison with that of 600 °C, and the monoclinic phase is formed to some extent.

The calcite peak exists from 500–700 °C, but gradually decreases with increasing temperature. This reveals the step in which calcite has decomposed into CaO and CO_2. Generally, the decomposition reaction of an isolated calcite occurs at 700–900 °C.

The major tetragonal phase and a little monoclinic phase coexist at 700–900 °C. However, the monoclinic phase becomes weaker at 1000 °C, and completely disappears at 1100 °C.

The appearance of $CaZrO_3$ is notable in the powders heated at 1000 °C. At 1100 °C, the tetragonal phase and $CaZrO_3$ phase coexist, but the $CaZrO_3$ phase becomes weaker. It seems that the decrease of $CaZrO_3$ is an indication of the transition of the tetragonal phase into cubic phase.

Thus, cubic zirconia solid solution is only formed above 1200 °C. From the high-angle XRD pattern, we can easily discriminate between tetragonal and cubic phases, as shown in Fig. 3, even though the angles of the diffraction peaks due to the cubic phase coincide with those due to the tetragonal phase in the low angles below $2\theta = 70^{\circ}$. The cubic phase was seen in the lower-angle side on the high-angle XRD patterns in the range $2\theta = 70^{\circ}$–78°. In Fig. 3, $(400)_c$ and $(400)_t$ denote the cubic phase and the tetragonal phase, respectively. From these results, it can be seen that the formation process of cubic zirconia solid solution passes through an intermediate stage with the formation of $CaZrO_3$.

Infrared spectra are quite dependent on the crystal structure and on the symmetry of the unit cell. The spectra develop additional bands as the crystal symmetry is lowered, and some of these bands are highly sensitive to the strain-induced distortions of the crystal lattice. The number of IR bands in the spectra increases as it transforms from the cubic phase to the tetragonal and monoclinic phases. IR spectra of the

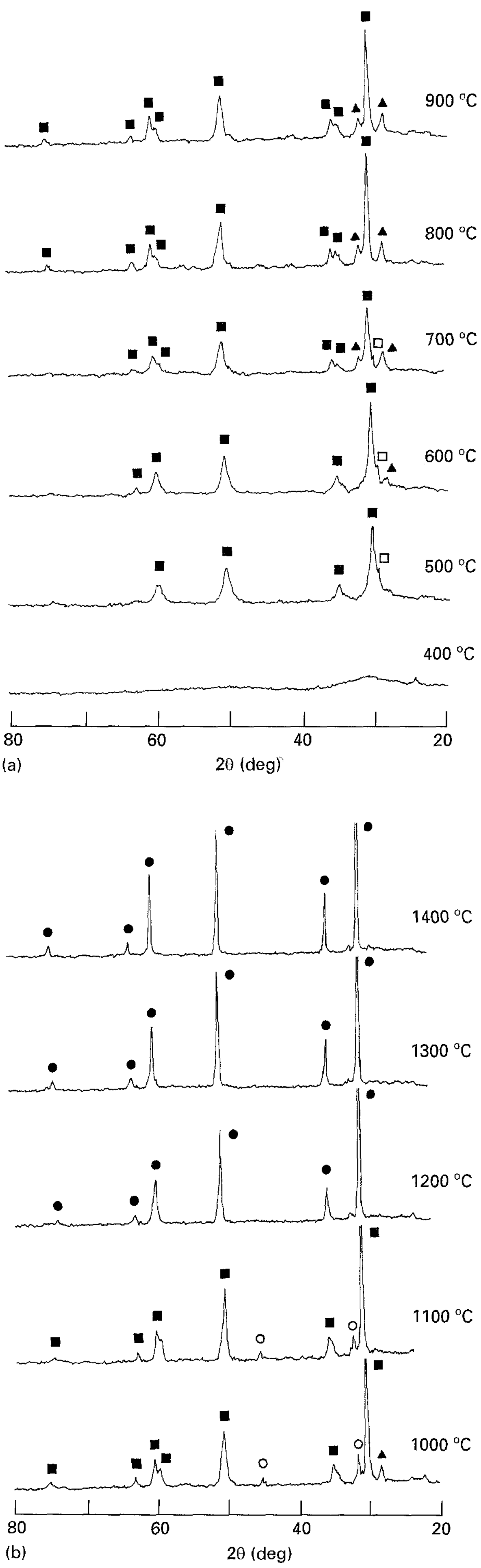

Figure 2 XRD patterns for powders calcined at (a) 400–900 °C, and (b) 1000–1400 °C. (●) cubic, (■) tetragonal, (▲) monoclinic, (○) $CaZrO_3$, (□) $CaCO_3$.

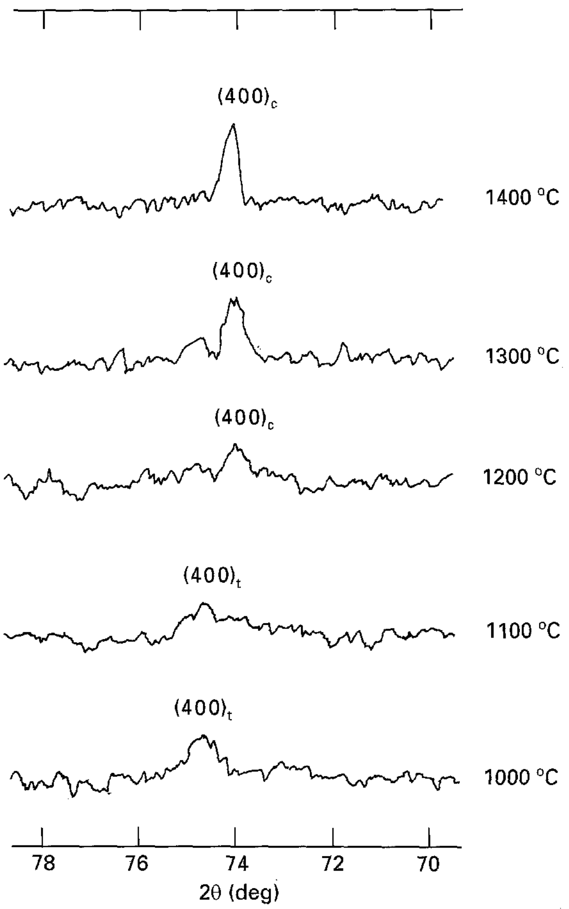

Figure 3 High-angle XRD patterns for the powders calcined at different temperatures from 1000–1400 °C.

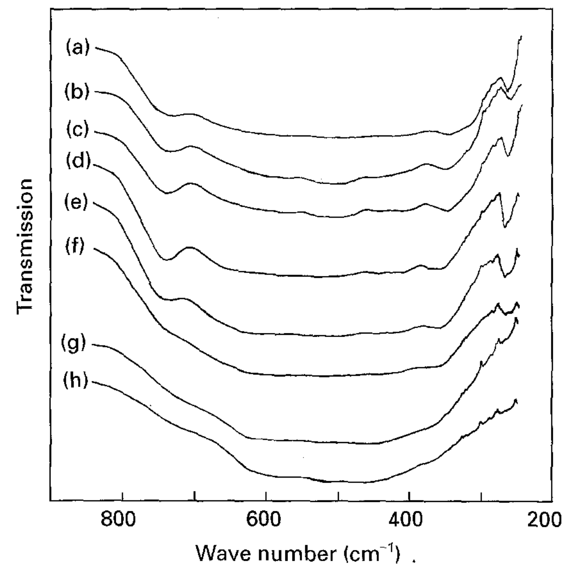

Figure 4 Infrared transmission spectra of the powders calcined at (a) 600 °C, (b) 700 °C, (c) 800 °C, (d) 900 °C, (e) 1000 °C, (f) 1100 °C, (g) 1200 °C, and (h) 1300 °C.

TABLE I Specific surface area and average particle size of the powders determined by the BET method

	Calcined powders			
Calcination temperature (°C)	Unmilled Surface area ($m^2 g^{-1}$)	Particle size (nm)	Milled Surface area ($m^2 g^{-1}$)	Particle size (nm)
700	58.4	18.2	88.5	12.0
800	49.9	21.3	58.3	18.2
900	35.2	30.3	38.9	27.3
1000	15.4	68.9	35.3	30.1

cubic and tetragonal phases are not especially distinctive, but the characteristic frequencies of the monoclinic phase are readily detected [4, 5]. McDevitt and Baun [4] clearly distinguished the IR spectra of the monoclinic and stabilized cubic phases of ZrO_2. At the same time, they showed that monoclinic samples with the same XRD pattern could have considerably different IR spectra. This suggests that IR spectra might be more sensitive than XRD patterns to small changes in the crystal lattice of the phases.

Fig. 4 illustrates the infrared transmission spectra of the powders calcined for 30 min at different temperatures from 600–1300 °C. Infrared transmission spectra were obtained from KBr pellets containing a powdered sample material of 0.67 wt %. The spectra were measured in the region 840–240 cm^{-1}, showing the fundamental vibrational frequencies in ZrO_2. The simple structures are observed with increasing temperature from above 1200 °C in Fig. 4, which are due to the stabilization of cubic phases. The spectrum of the stabilized cubic phase shows the fundamental band near 480 cm^{-1} and weak broad bands at its high- and low-frequency sides [5].

The structures become more pronounced in the lowest temperature region in which the tetragonal phase is dominant (curve (a)). Strong bands around 740 and 270 cm^{-1}, illustrating the characteristic features of monoclinic phase [5], are observed in the low-temperature region from 600–1000 °C. An orderly progression of the bands is observed with increasing temperature up to 900 °C. Changes in the basic character of these spectra are in agreement with the previous XRD data. The XRD data of the powders calcined up to 1000 °C showed the tetragonal phase with a small amount of monoclinic phase, whereas the powder calcined at 1200 °C was pure cubic.

When tetragonal ZrO_2 and monoclinic ZrO_2 coexist in XRD data, the fractions of the two phases in the sample can be quantitatively determined by the polymorph method of Garvie and Nicholson [6]. From these results, it can be shown that the tetragonal phases decrease slightly with increasing heating temperatures in the low-temperature regions, whereas the tetragonal phases increase at 1000 °C. In particular, it is observed that the tetragonal phases exist in the calcined powder at 1000 °C, even though the particle size of the powder is larger than the critical size of 30 nm (see Table I), above which the metastable tetragonal phase of pure ZrO_2 cannot exist at room temperature as a result of the crystallite size effect [7]. This is the result of the stabilization of tetragonal phases in the calcined powder at 1000 °C which may be due to the alloying effect by the addition of an appropriate amount of stabilizer. It is well known that the addition of calcia to zirconia to form a solid solution reduces the transformation temperature [8].

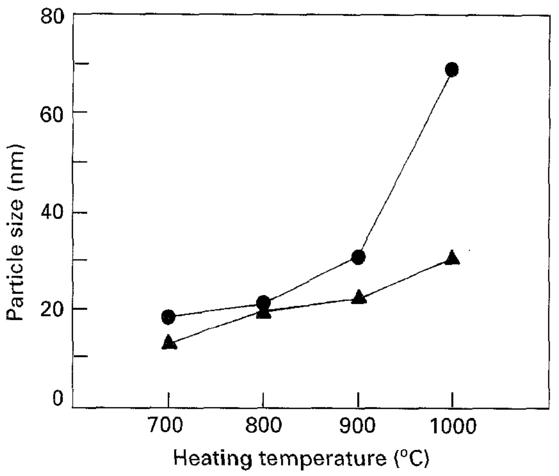

Figure 5 Particle (crystallite) size versus calcination temperature. (●) BET method, (▲) XRD-LB method.

The specific surface area and the average particle size of the calcined powders with and without milling are listed in Table I. The specific surface area was measured by the multipoint BET method, and then the average particle size was calculated. The specific surface area decreases apparently with increasing heat-treatment temperature. The corresponding increase in the average particle size is shown.

Fig. 5 shows a comparison of the particle (crystallite) size obtained by the BET and XRD-LB methods. Both methods reveal comparable particle size in the lower temperature region, but there is an inconsistency at the high temperature of 1000 °C. At 1000 °C, the particle size calculated from the BET data is larger than the crystallite size found by the XRD-LB method. This phenomenon may be due to the following reason. In the case of the high-temperature calcined powders the absorption gas of BET measurement has difficulty penetrating into the agglomerated powders with an open arrangement of crystallites. In fact, the size of particles calcined at 1000 °C is remarkably reduced by milling, as shown in Table I. In addition, the crystallite size cannot conceptually be larger than the primary particle size. It is observed in the figure that the particle (crystallite) size increases with increase in the calcination temperature, which is in agreement with the particle growth with increasing temperature.

In the BET results of Table I, the surface area of the milled calcined powders is considerably increased compared to the unmilled powders. This indicates the reduction of the agglomerates, which are the secondary particles. Agglomerates are formed in the early stages of the preparation process and transformed to strong agglomerates during heat treatments such as drying and calcination. It is well known that agglomerates lead to a reduction of the green density, interfere in the development of microstructure, and impede the sintering kinetics [9]. Consequently, a high sintered density with reduced sintering temperatures and/or times can be achieved by the elimination or reduction of the agglomerates.

Scott and Reed [10] obtained the submicrometre-sized yttria-stabilized zirconia with a density $> 99.5\%$,

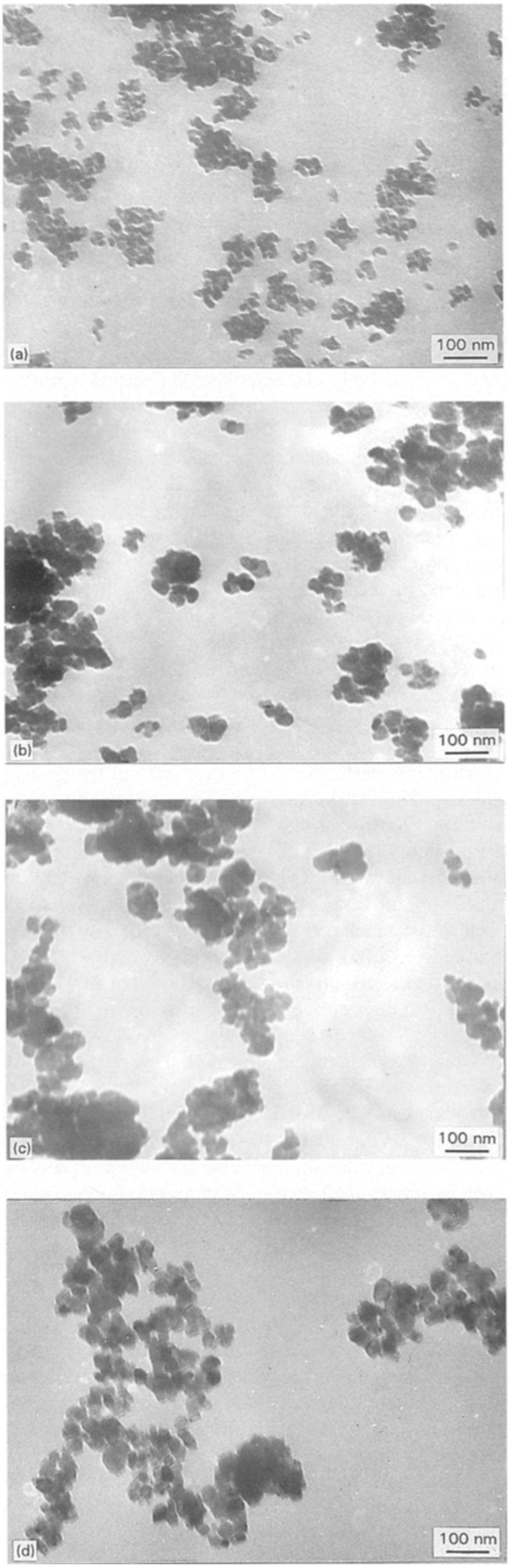

Figure 6 Transmission electron micrographs of the powders calcined at different temperatures: (a) 700 °C, (b) 800 °C, (c) 900 °C and (d) 1000 °C.

by using the milling and laundering processes. They showed that milling and deagglomeration enhanced sintering in the final stage, and compacts of laundered, milled and deagglomerated powders attained an ultimate density at a temperature 150 °C lower than for compacts of as-received power.

A comprehensive investigation of the agglomerate and particle size effects on sintering yttria-stabilized zirconia was also reported by Rhodes [9]. He showed that an agglomerate-free powder was sintered to 99.5% theoretical density at 1100 °C, which is $\approx$300 °C lower than necessary for an agglomerated but equal crystallite size powder.

Haberko [2] also studied the dependence of powder and sintered body characteristics on washing procedures, in order to prevent the formation of strong particle agglomerates. Calcination of gels washed with alcohol resulted in a powder composed of agglomerates which were much more porous and by themselves mechanically weaker than agglomerates obtained from gels washed with water. A high relative density of 98% at a sintering temperature as low as 1300 °C has been achieved by using the powders washed with alcohol.

In order to suppress the formation of hard agglomerates, a washing process with ethyl alcohol, a stirring process during washing, and a milling process after calcination, were employed in the present studies. The reduction of agglomerates by means of milling was observed, as shown in Table I. In sintering behaviour experiments performed as an extension of the present work, high relative densities were obtained at low sintering temperatures [11]. Fine powders washed with alcohol and ball-milled after calcination at 800 °C were used. Compaction was performed at a pressure of 1000 kg cm^{-2} using a uniaxial press, and sintering was carried out for 5 h at different temperatures from 1100–1400 °C at intervals of 100 °C. The experimental results showed that a value of $> 92\%$ theoretical density was attained at a low temperature of 1200 °C.

Table I reveals that the particle sizes of the milling and screened powders become larger from 12 nm at 700 °C up to 30 nm at 1000 °C. Fig. 6 shows transmission electron micrographs of the milled calcined powders. It can be seen that the particles grow with increasing heat-treatment temperature. The corresponding values with the BET measurements in the average particle size are shown.

The three methods of particle size determination applied in the present studies yield approximately the same value of particle size. The coincidence between the BET particle size with milling and the crystallite size, obtained from the XRD-LB method, indicates that the calcined powders are composed of isometric crystallites. This result is confirmed by the transmission electron micrographs.

4. Conclusions

13 mol % calcia-stabilized zirconia powders for oxygen ionic conductors were synthesized by the coprecipitation method. The characterization of powders has been investigated using TG and DTA for thermal analysis, XRD and IR for crystalline phase identification, and BET, XRD-LB, and TEM for particle size and morphology determination. From the above results, the following conclusions can be drawn.

1. The precipitates had a specific surface area of 193 $m^2 g^{-1}$, and appeared to be the fine and spherical primary particles with a size of approximately 5 nm.
2. The tetragonal phase was stable in the low calcination temperature regions, and the cubic zirconia solid solution was formed from above 1200° C through an intermediate stage of the formation of $CaZrO_3$.
3. The particle size of the calcined powders increased with increasing calcination temperature, and the specific surface area was increased by milling.
4. The powders obtained by this method had a great reactivity. With these powders, it was possible to attain a value of $> 92\%$ theoretical density at a temperature of 1200 °C.

Acknowledgements

The authors thank Dr Y.B. Kim for the IR measurements. This work was supported by the Kyung-Sung University and the Ministry of Education of Korea through the Research Fund for Advanced Materials in 1994.

References

1. R. J. BROOK, in "Advances in Ceramics", Vol. 3, edited by A. H. Heuer and L. W. Hobbs (American Ceramic Society, Columbus, OH, 1981) p. 272.
2. K. HABERKO, *Ceram. Int.* **5** (1979) 148.
3. A. ROOSEN and H. HAUSNER, in "Ceramic Powders", edited by P. Vincenzini (Elsevier Scientific, Amsterdam, 1983) p. 773.
4. N. T. McDEVITT and W. L. BAUN, *J. Am. Ceram. Soc.* **47** (1964) 622.
5. C. M. PHILLIPPI and K. S. MAZDIYASNI, *ibid.* **54** (1971) 254.
6. R. C. GARVIE and P. S. NICHOLSON, *ibid.* **55** (1972) 303.
7. R. C. GARVIE, *J. Phys. Chem.* **69** (1965) 1238.
8. V. S. STUBICAN, in "Advances in Ceramics", Vol. 24A, edited by S. Sōmiya, N. Yamamoto and H. Yanagida (American Ceramic Society, Westerville, OH, 1988) p. 71.
9. W. H. RHODES, *J. Am. Ceram. Soc.* **64** (1981) 19.
10. C. E. SCOTT and J. S. REED, *Ceram. Bull.* **58** (1979) 587.
11. J. I. PARK, J. S. LEE and T. W. CHOI to be submitted.

Received 23 June
and accepted 25 October 1995